Journal of Engineering Science and Technology
Vol. 14, No. 2 (2019) 1101 - 1117

MITIGATION OF SUB-SYNCHRONOUS RESONANCE WITH STATIC VAR COMPENSATOR

NILAYKUMAR A. PATEL[1,*], PRAGHNESH BHATT[2]

[1]Electrical Engineering Department, Chandubhai S Patel Institute of Technology, CHARUSAT University, CHARUSAT Campus, Changa, Gujarat, 388421, India
[2]Department of Electrical Engineering, School of Technology, Pandit Deendayal Petroleum University, Raisan, Gandhinagar, India
*Corresponding Author: nilaypatel.cem@charusat.ac.in

Abstract

The rapid growth of the power sector and emergence leads towards bulk power transfer over long transmission lines. This issue demands series compensation of transmission line. Series compensation of transmission line not only enhances the stability of the power system but also may potentially lead the system towards the problem of Subsynchronous-Resonance (SSR). This paper presents the detailed small signal model of IEEE First Benchmark Model (FBM) for eigenvalue analysis in order to identify responsible modes of oscillations for SSR. To mitigate SSR, the application of Static Var Compensator (SVC) located in the transmission line has been investigated. Two individual supplementary control strategies, namely generator terminal voltage deviation and generator rotor speed deviation, for SVC have been implemented. The coordinated operation of the power system stabilizer in the generator control loop and terminal voltage deviation as a supplementary signal for SVC is tested in this paper. It is found that the combined operation can successfully mitigate SSR and stabilize the system with a high degree of series compensation.

Keywords: Eigenvalues, IEEE FBM, Series compensation, Static VAR compensator, Subsynchronous resonance.

1. Introduction

The different masses of turbine-generators shafts are much susceptible to interaction with the electrical resonances of a transmission network, which is compensated with conventional series capacitors. This can lead to a form of instability known as Subsynchronous Resonance (SSR), which can result in failure of turbine-generator shafts [1, 2]. Extensive research has been started to understanding SSR phenomenon after two successive shaft failures incidences reported at Mohave power plant in USA in 1970 and 1971. There are two main characteristics of SSR phenomenon, namely, (a) self-excitation (also known as steady state SSR) and (b) transient torques (also known as transient SSR) [1-5]. The currents entering generator terminals and oscillating with sub-synchronous frequency produce sub-synchronous frequency voltage components at generator terminal. These voltages can sustain sub-synchronous frequency currents to produce the effect that is termed as self-excitation, which is further categorized into two categories: (i) Induction Generator Effect (IGE) and (ii) Torsional Interaction (TI). In IGE, only rotor electrical dynamics is involved whereas TI deals with both rotors electrical and mechanical dynamics.

The system disturbances such as sudden load changes, faults or tripping of the lines can excite oscillatory torques on the generator rotor. The transient oscillatory electrical torques thus produced may have unidirectional, exponentially decaying as well as oscillatory torques components ranging from sub-synchronous to multiples of network frequency. The sub-synchronous frequency components of torques with large amplitudes just after the disturbance affect the shaft life due to fatigue damage and are analyzed under transient SSR phenomena. Several mitigation techniques for SSR mitigation such as blocking filters using static circuitry, excitation controllers using supplementary signals, torsional relays and many others are reported in the literature [5]. Kumar and Kumar [6] commented, line current and active power-based controller are used for SSR mitigation using SVC. According to Padiyar and Varma [7], damping torque investigation of SMIB system has been presented with SVC located at mid-way of the transmission line. SVCs are basically used for bus voltage regulation. However, SVC output using some supplementary signals can be used to mitigate and damp out power system oscillations [8-12]. Zhijun et al. [13] and Jovcic et al. [14] presented the dynamic phasor and analytical model of SVC. Jusan et al. [15] also described the SSR study using SVC, where the front and rear speeds of HP stage of turbine and exciter, respectively. Wasynczuk [12] earlier addressed this is used as control concept. Zhu et al. [16] explained that the rotor angle deviation signal as a supplementary control signal has been used along with reactive power control loop of unified power flow controller to damp out oscillation caused by subsynchronous resonance. Based on studies by Panda et al. [17], the similar approach is used, but here supplementary signal is used for static synchronous series compensator along with main control loop for effective damping of SSR. Nagarajan and Kumar [18] highlighted that the fuzzy logic control of static VAR system is described; also, the superiority of static VAR system is explained with respect to reactive power generation and absorption. Sreeranganayakulu et al. [19] explained that the effectiveness of SVC is proved using IEEE second benchmark model, but here the linearized model is not tested.

In this paper, systematic mathematical modelling of IEEE FBM model has been formulated with the linearized equation to carry out eigenvalue analysis. The generator model of basic benchmark system has been modified to incorporate

modelling of Automatic Voltage Regulator (AVR) and Power System Stabilizer (PSS). In addition to that, compressive SVC model has been prepared and an attempt is made to mitigate SSR using two different supplementary signals. In all previous work, the modelling of AVR and PSS are not included, also the comprehensive linearized modelling of SVC with its control part are not included.

2. Power System Modelling for SSR Studies

Figure 1 shows IEEE First Benchmark Model (FBM) for the analysis of SSR [2]. The test system data utilized in this paper is described in *Appendix A*. Before representing the modelling of SVC to mitigate SSR, the turbine-generator models, excitation system and electrical network interfacing with series compensation are modelled to carry out SSR without considering SVC. The formulation of state equations first starts with individual component modelling, which subsequently integrated to form overall combined state space systems for the computation of eigenvalues of the entire network to represent different modes of oscillations.

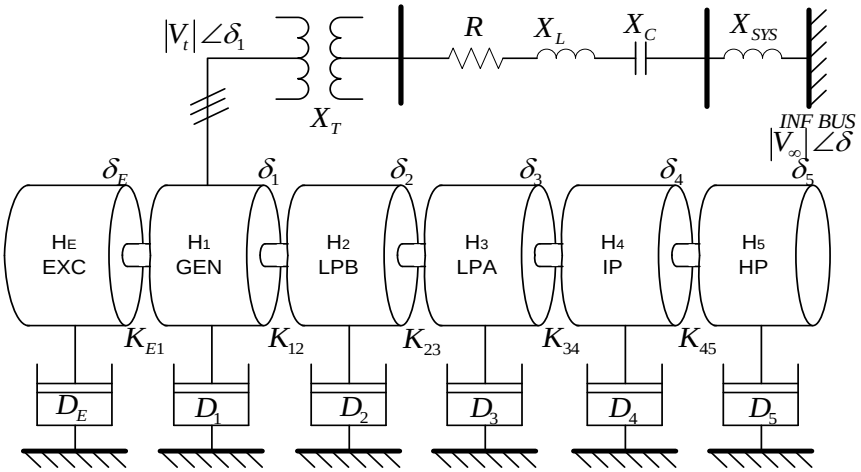

Fig. 1. Turbine-Generator shaft representation along with network as per IEEE FBM.

2.1. Modelling of synchronous generator

Type 2.2 model of the synchronous machine is used in this work. This model of synchronous machine has one field winding (f_d) and one damper windings (k_d) on d-axis of rotor whereas two damper windings (k_{q1} and k_{q2}) on q-axis of the rotor [20]. The state space equations for the synchronous generator is given as per Eq. (1) using flux linkage dynamics of stator and rotor windings as state variables.

$$\frac{d}{dt}\Delta x_e = [A_e]\Delta x_e + [B_{eN}]\begin{bmatrix}\Delta V_{tq}\\ \Delta V_{td}\end{bmatrix} + [B_{eM}]\Delta\omega + [B_{eP}]\begin{bmatrix}\Delta V_{kq1}\\ \Delta V_{kq2}\\ \Delta e_{xfd}\\ \Delta V_{kd}\end{bmatrix} \quad (1)$$

where

$$\Delta x_e^T = \left[\Delta\psi_{qs} \quad \Delta\psi_{ds} \quad \Delta\psi_{kq1} \quad \Delta\psi_{kq2} \quad \Delta\psi_{fd} \quad \Delta\psi_{kd} \right]$$

and Δ represents a small change in quantities.

Other matrices are listed in *Appendix B*.

2.2. Modelling of turbine-generator unit-mechanical system

The turbine–generator unit considered as lumped masses forms the mechanical system and it consists of six masses of different pressure stages as shown in Fig. 1 [2]. The synchronous generator and an exciter are also coupled on the same shaft. The state equation for a mechanical system is given in per unit as per Eq. (2). In the presented mechanical system, there are total twelve state variables of mechanical systems including six of speed deviation of each masses and another six are angular position of each masses.

$$[2H]\, p\underline{\omega} + [D]\underline{\omega} + [K] + \underline{T} = 0 \tag{2}$$

where the shaft stiffness matrix is denoted by [*K*]. The [*H*] and [*D*] matrices are diagonal matrix of inertias and damping constants, respectively. T gives torque vector acting on the different pressure stages of shaft and ω is the speed vector. The inertia constants and shaft stiffness of different stages are given in *Appendix A*. Damping is ignored in presented work.

2.3. Electrical network interfacing

The electrical equivalent circuit for the IEEE first benchmark model to study SSR is shown in Fig. 2. The generator with constant voltage source E_g is connected to the an infinite bus through series compensated transmission line. The terminal voltage of the generator is V_t.

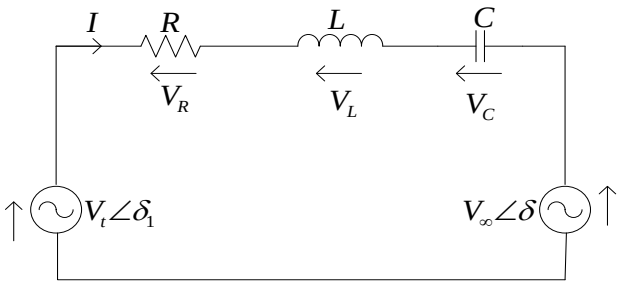

Fig. 2. Network model of FBM.

The state equations of electrical network in d–q components are given as per Eqs. (3) and (4).

$$\left.\begin{aligned} V_{td} &= Ri_d + \frac{X_L}{\omega_0} pi_d - \frac{\omega}{\omega_0} X_L i_q + v_{cd} + V_\infty \sin\delta \\ V_{tq} &= Ri_q + \frac{X_L}{\omega_0} pi_q + \frac{\omega}{\omega_0} X_L i_d + v_{cq} + V_\infty \cos\delta \end{aligned}\right\} \tag{3}$$

$$\left.\begin{aligned} pv_{cd} &= \omega v_{cq} + \omega_0 X_C i_d \\ pv_{cq} &= -\omega v_{cd} + \omega_0 X_C i_q \end{aligned}\right\} \tag{4}$$

2.4. Integration of system components

The set of state space Eqs. (1) to (4) of individual components are integrated to formulate the state equations of the overall system in order to capture the different dynamic events related to SSR. The dimensions of A matrix of the integrated system consist of a generator, mechanical masses and the network is of 20×20.

3. Network Model with SVC

The main component of the SVC is the parallel combination of Fixed Capacitor (FC) and Thyristor-Controlled Reactor (TCR). Figure 3 shows the presence of SVC at the predetermined location of the line. The location of SVC is ascertained by considering equivalent values of line impedance R_1+jwL_1 and $R_2 + jwL_2$. The state space equations after incorporating SVC are formulated as per Eqs. (5) to (10).

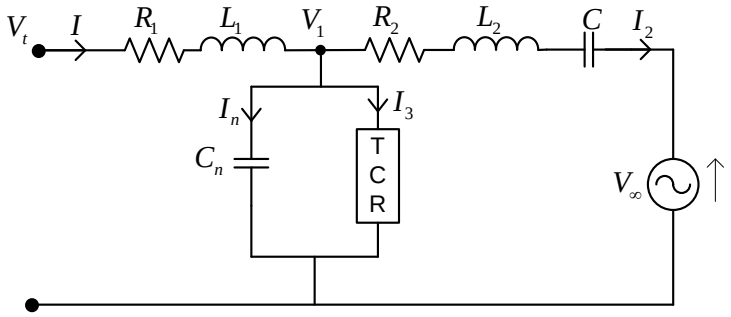

Fig. 3. Network model with SVC.

The voltages in d-q frame at location of SVC are given by Eqs. (5) and (6) and voltages across series capacitor are represented by Eqs. (7) and (8).

$$V_{1q} = R_2 i_{2q} + \frac{X_{L2}}{\omega_0} p i_{2q} + \frac{\omega}{\omega_0} X_{L2} i_{2d} + V_{cq} + V_\infty \cos\delta \tag{5}$$

$$V_{1d} = R_2 i_{2d} + \frac{X_{L2}}{\omega_0} p i_{2d} - \frac{\omega}{\omega_0} X_{L2} i_{2q} + V_{cd} + V_\infty \sin\delta \tag{6}$$

$$pV_{cq} = -\omega V_{cd} + \omega_0 X_c i_{2q} \tag{7}$$

$$pV_{cd} = \omega V_{cq} + \omega_0 X_c i_{2d} \tag{8}$$

The voltages V_1 at the location of SVC in d-q frame are represented below.

$$C_n pV_{1q} + \omega C_n V_{1d} = I_q - I_{3q} - I_{2q} \tag{9}$$

$$C_n pV_{1d} - \omega C_n V_{1q} = I_d - I_{3d} - I_{2d} \tag{10}$$

The set of Eqs. (5) to (10) in linearized form are obtained to form the state equation in terms of the voltage across the series capacitor and the current flowing through it as well as the voltage at SVC terminal.

$$p\begin{bmatrix}\Delta i_{2q}\\ \Delta i_{2d}\\ \Delta V_{cq}\\ \Delta V_{cd}\\ \Delta V_{1q}\\ \Delta V_{1d}\end{bmatrix}=\begin{bmatrix}-\frac{\omega_0}{X_{L2}}R_2 & -\omega_0 & -\frac{\omega_0}{X_{L2}} & 0 & \frac{\omega_0}{X_{L2}} & 0\\ \omega_0 & -\frac{\omega_0}{X_{L2}}R_2 & 0 & -\frac{\omega_0}{X_{L2}} & 0 & \frac{\omega_0}{X_{L2}}\\ \omega_0 X_c & 0 & 0 & -\omega_0 & 0 & 0\\ 0 & \omega_0 X_c & \omega_0 & 0 & 0 & 0\\ -\omega_0 X_{cn} & 0 & 0 & 0 & 0 & -\omega_0\\ 0 & -\omega_0 X_{cn} & 0 & 0 & \omega_0 & 0\end{bmatrix}\begin{bmatrix}\Delta i_{2q}\\ \Delta i_{2d}\\ \Delta V_{cq}\\ \Delta V_{cd}\\ \Delta V_{1q}\\ \Delta V_{1d}\end{bmatrix} \tag{11}$$

$$+\begin{bmatrix}-I_{2d0} & \frac{\omega_0}{X_{L2}}V_\infty\sin\delta_0\\ I_{2q0} & -\frac{\omega_0}{X_{L2}}V_\infty\cos\delta_0\\ -V_{cd0} & 0\\ V_{cq0} & 0\\ -V_{1d0} & 0\\ V_{1q0} & 0\end{bmatrix}\begin{bmatrix}\Delta\omega\\ \Delta\delta\end{bmatrix}+\begin{bmatrix}0 & 0\\ 0 & 0\\ 0 & 0\\ 0 & 0\\ -\omega_0 X_{cn} & 0\\ 0 & -\omega_0 X_{cn}\end{bmatrix}\begin{bmatrix}\Delta i_{3q}\\ \Delta i_{3d}\end{bmatrix}+\begin{bmatrix}0 & 0\\ 0 & 0\\ 0 & 0\\ 0 & 0\\ \omega_0 X_{cn} & 0\\ 0 & \omega_0 X_{cn}\end{bmatrix}\begin{bmatrix}\Delta i_q\\ \Delta i_d\end{bmatrix}$$

Similarly, voltage differences between generator terminal and SVC location are given in Eqs. (12) and (13).

$$V_{tq}-V_{1q}=R_1 i_q+\frac{X_{L1}}{\omega_0}pi_q+\frac{\omega}{\omega_0}X_{L1}i_d \tag{12}$$

$$V_{td}-V_{1d}=R_1 i_d+\frac{X_{L1}}{\omega_0}pi_d-\frac{\omega}{\omega_0}X_{L1}i_q \tag{13}$$

Using the linearized value of above mentioned V_{tq} and V_{td} into Eq. (1), the linearized state equations of stator and rotor flux linkages can be formed.

The current I_3 through reactor of SVC in Fig. 3 can be modeled by considering only the reactance Ls as below after neglecting its resistance Rs.

$$V_{1q}=L_S pi_{3q}+\omega L_S i_{3d}=\frac{X_{LS}}{\omega_0}pi_{3q}+\frac{\omega X_{LS}}{\omega_0}i_{3d} \tag{14}$$

$$V_{1d}=L_S pi_{3d}-\omega L_S i_{3q}=\frac{X_{LS}}{\omega_0}pi_{3d}-\frac{\omega X_{LS}}{\omega_0}i_{3q} \tag{15}$$

Linearizing and rearranging, we have:

$$p\Delta i_{3q}=\omega_0 V_{1q0}\Delta B+\omega_0 B_0\Delta V_{1q}-\omega_0\Delta i_{3d}-i_{3d0}\Delta\omega \tag{16}$$

$$p\Delta i_{3d}=\omega_0 V_{1d0}\Delta B+\omega_0 B_0\Delta V_{1d}+\omega_0\Delta i_{3q}+i_{3q0}\Delta\omega \tag{17}$$

Control of SVC

The small signal model for SVC control to be used for SSR mitigation is shown in Fig. 4. The perturbation in terminal voltage at SVC location and current through

TCR in Fig. 3 are fed to the reference point. The measurement time constant for both voltage and current is assumed to be equal and represented by T_m. PI control block acts as a voltage regulator. Firing delay time and average dead time are given by T_D and T_S, respectively. These parameters values are listed in *Appendix A*. The feedback signal of voltage perturbation changes the susceptance. ΔV_F may be used as a supplementary feedback signal, it is ignored at present.

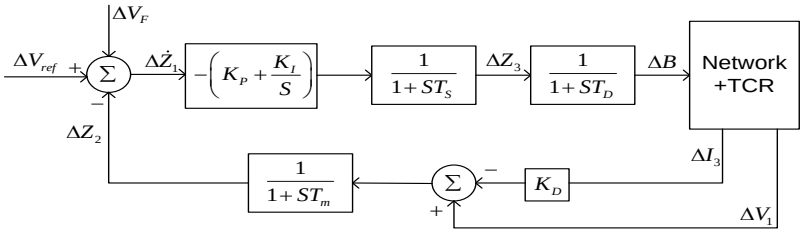

Fig. 4. Control of SVC for SSR mitigation.

The dynamic equations of SVC compensated network using the notations used in Fig. 4 are as follows.

$$p\Delta Z_1 = \Delta V_{ref} - \Delta Z_2 + \Delta V_F \tag{18}$$

where V_F is for supplementary feedback signal, which has been ignored.

$$p\Delta Z_2 = \frac{1}{T_m}\left(\Delta V_1 - K_D \Delta i_3\right) - \frac{1}{T_m}\Delta Z_2 \tag{19}$$

$$\Delta V_1 = \frac{V_{1d0}}{V_{10}}\Delta V_{1d} + \frac{V_{1q0}}{V_{10}}\Delta V_{1q} \tag{20}$$

Similarly,

$$\Delta i_3 = \frac{i_{3d0}}{i_{30}}\Delta i_{3d} + \frac{i_{3q0}}{i_{30}}\Delta i_{3q} \tag{21}$$

From Eqs. (19), (20) and (21), the following equation is obtained,

$$p\Delta Z_2 = \frac{1}{T_m}\left[\frac{V_{1d0}}{V_{10}}\Delta V_{1d} + \frac{V_{1q0}}{V_{10}}\Delta V_{1q} - K_D\left(\frac{i_{3d0}}{i_{30}}\Delta i_{3d} + \frac{i_{3q0}}{i_{30}}\Delta i_{3q}\right)\right] - \frac{1}{T_m}\Delta Z_2 \tag{22}$$

Other state variable linearized equations are,

$$p\Delta Z_3 = -\frac{K_I}{T_S}\Delta Z_1 + \frac{K_P}{T_S}\Delta Z_2 - \frac{1}{T_S}\Delta Z_3 - \frac{K_P}{T_S}\Delta V_{ref} - \frac{K_P}{T_S}\Delta V_F \tag{23}$$

$$p\Delta B = \frac{\Delta Z_3}{T_D} - \frac{\Delta B}{T_D} \tag{24}$$

The matrix for control diagram equations is obtaining using Eqs. (16) to (18) and (22) to (24). The total state variable of the system with the SVC and its control will be thirty. Hence, the A matrix will be of the order of 30×30.

4. Modelling of AVR and PSS

The use of AVR is needed for the synchronous generator to restore its terminal voltage automatically in the event of load changes or fault condition. To make a response of AVR faster, the gain K_A of PSS is set to a higher value, which in turn reduces the damping torque of the system.

When the system is working at higher loading conditions and the synchronous generator is connected to load through a larger reactance, the use of AVR can result in negative damping torque in the system and the system may become oscillatory unstable. To avoid oscillatory instability and to compensate for negative damping torque effect of AVR, PSS as shown in Fig. 5 is used. PSS can provide the necessary phase shift through its lead-lag blocks depending on the requirement and can successfully make the system stable.

Total five state variables will be added in the system with the addition of AVR and PSS. The state equation of AVR and PSS are not listed here, it can be easily derived from its block diagram figure. After addition of AVR and PSS into the test system, the total state variable will be thirty-five.

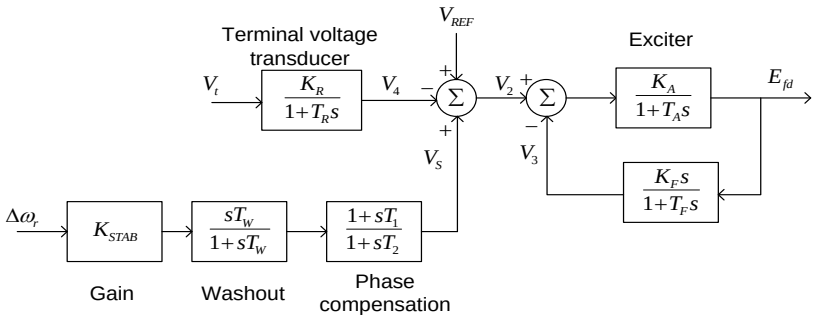

Fig. 5. Block diagram of AVR and PSS.

5. Use of Supplementary Signal for Mitigation of SSR

5.1. Rotor speed deviation as a supplementary signal

Here rotor speed deviation is taken as a supplementary signal to mitigate SSR. The block diagram of the transfer function is given in Fig. 6.

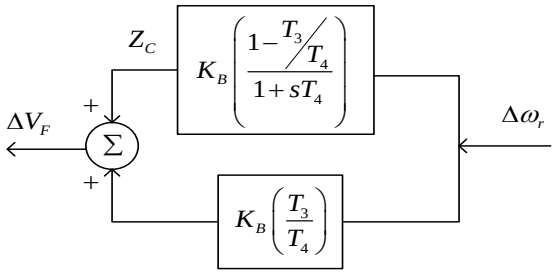

Fig. 6. Transfer function block diagram of supplementary signal as rotor speed deviation.

The equations derived from Fig. 6 are as follows.

$$pZ_C = -\frac{1}{T_4}Z_C + \left[\frac{K_B}{T_4}\left(1-\frac{T_3}{T_4}\right)\right]\Delta\omega_r \tag{25}$$

$$V_F = K_B\left(\frac{T_3}{T_4}\right)\Delta\omega_r + Z_C \tag{26}$$

Incorporating above equations, we have now total thirty-six state variables, hence the A matrix of state space equation will be 36×36.

5.2. Generator terminal voltage deviation as a supplementary signal

Here generator terminal voltage deviation is taken as a supplementary signal to mitigate SSR. The block diagram of the transfer function is given in Fig. 7.

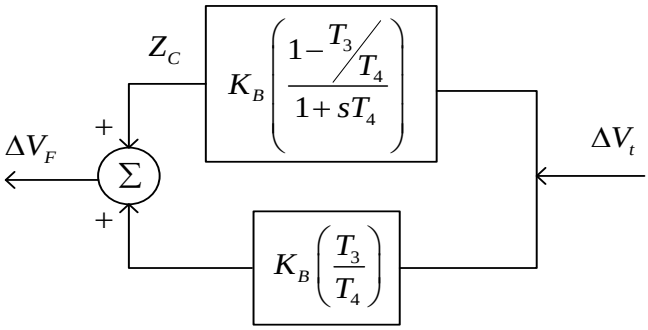

Fig. 7. Transfer function block diagram of supplementary signal as generator terminal voltage deviation.

The equations derived from Fig. 7 are as follows.

$$pZ_C = -\frac{1}{T_4}Z_C + \left[\frac{K_B}{T_4}\frac{E_{q0}}{E_0}\left(1-\frac{T_3}{T_4}\right) \quad \frac{K_B}{T_4}\frac{E_{d0}}{E_0}\left(1-\frac{T_3}{T_4}\right)\right]\begin{bmatrix}\Delta V_{tq}\\ \Delta V_{td}\end{bmatrix} \tag{27}$$

$$p\Delta V_F = -\frac{\Delta V_F}{T_4} + C_1\begin{bmatrix}\Delta V_{tq}\\ \Delta V_{td}\end{bmatrix} + C_2\frac{d}{dt}\begin{bmatrix}\Delta V_{tq}\\ \Delta V_{td}\end{bmatrix} \tag{28}$$

where,

$$C_1 = \frac{K_B}{T_4}\left[\frac{V_{tq0}}{V_{t0}} \quad \frac{V_{td0}}{V_{t0}}\right]$$

$$C_2 = K_B\left(\frac{T_3}{T_4}\right)\left[\frac{V_{tq0}}{V_{t0}} \quad \frac{V_{td0}}{V_{t0}}\right]$$

Incorporating above equations in the system discussed in section IV, we have now total thirty-six state variables, hence the A matrix of state space equation will be 36×36.

6. Results and Discussion

In this paper, the various state space equations formulation is categorized in different cases as below.

Case I: The overall base system explained in Section II.

Case II: Inclusion of SVC in case I system.

Case III: Inclusion of AVR and PSS in case II system.

Case IV:
(a) Addition of rotor speed deviation as a supplementary signal in case III system.
(b) Addition of generator terminal voltage deviation as a supplementary signal in case III system.

The data used for SSR analysis with IEEE FBM shown in Fig. 2 are given in *Appendix A*. The series compensation level considered in this work is equal to 50%, i.e., the total inductive reactance (including transformer and transmission line) is compensated by 50% by incorporating capacitive compensation. The objectives of the work are to carry out eigenvalue analysis for all above-listed cases and to investigate the effect of series compensation on SSR.

The eigenvalue analyses for first three cases have been reported in Table 1 to identify the torsional modes, which have the frequency of oscillations in a sub-synchronous frequency range. Some torsional modes are highlighted, which have the positive real part, which is responsible to create subsynchronous resonance in the system. The real part of eigenvalues must be negative for stable operation. In Table 1, some eigenvalues of torsional modes have positive real values; hence this case situation leads towards the subsynchronous resonance. The use of SVC can improve one of the torsional modes as compared to the base system but not fully succeed to mitigate SSR. The addition of AVR and PSS in the generator control loop can improve the torsional mode but left the system with insufficient damping, which can be noticed through larger real part of eigenvalues related to modes of rotor windings.

Hence, it is observed that the system with SVC in transmission network and utilizing AVR and PSS in generator control loop are unable to mitigate the torsional oscillations when the system is compensated with a series capacitor. In order to mitigate the impact of SSR and to stabilize the system with series compensation, the application of two different supplementary signals has been explored. Table 2 shows the performance of the system after using two

supplementary signals. The use of rotor speed deviation is still not capable to mitigate SSR because it has some eigenvalues with positive real parts, but it can be noticed from Table 2 that the use of generator terminal voltage deviation as a supplementary signal can successfully mitigate all torsional modes and make the system stable. All eigenvalues show the negative real parts and result in higher damping even with 50% compensation level.

Time domain simulations are also carried out for case III and case IV(b) in MATLAB-Simulink using derived equations. Figures 8 and 9 show the time domain response of oscillations of masses and the shaft torque between LPA and LPB turbine for the disturbance applied at t = 6 seconds for case III and case IV(b) respectively. The results of time domain simulations validate the results obtained from the eigenvalue analysis.

Table 1. Results of eigenvalue analysis for case I to III.

IEEE FBM with 50% series compensation (Case I)	IEEE FBM 50% series compensation + SVC installed on transmission line (Case II)	IEEE FBM SVC+AVR-PSS (Case III)	Modes of oscillations
-4.716 ± 623.63i	-6.063 ± 376.945i -2.454 ± 704.320i -4.074 ± 879.601i	-5.88 ± 376.84i -2.589 ± 698.90i -4.109 ± 894.575i	Supersynchronous mode
± 297.97i	± 297.97i	± 297.97i	Torsional mode
± 202.84i	-0.009 ± 202.804i	-0.062 ± 202.79i	Torsional mode
± 160.50i	-0.016 ± 160.41i	-0.08 ± 160.34i	Torsional mode
0.0004 ± 126.94i	**0.143 ± 126.798i**	-0.043 ± 127.01i	Torsional mode
0.001 ± 98.70i	0.405 ± 99.030i	**0.05 ± 98.85i**	Torsional mode
-2.636 ± 130.35i	-1.987 ± 49.455i -4.689 ± 125.255i	-34.816 ± 29.956i -3.423 ± 54.211i -3.719 ± 139.747i	Subsynchronous mode
0.0013571638373	**0.990 ± 11.870i**	-101.12 ± 3.78i	Swing mode
0 -0.998 -4.4399 -20.467 -33.194	-3.498 ± 0.793i -0.283 -20.441 -33.897 -92.627 -16.608, -130.121	-4.79 ± 1.58i -0.225, -0.462 -1.309 **4.698, 9.971** -20.459, -58.157 -114.783 -1000.20	Modes related to damper winding, field winding and SVC.

Table 2. Results of eigenvalue analysis for case IV.

IEEE FBM SVC+AVR-PSS rotor speed deviation as a supplementary signal (Case IV-a)	IEEE FBM SVC+AVR-PSS generator terminal voltage as a supplementary signal (Case IV-b)	Modes of oscillations
-3.395 ± 375.80i -3.192 ± 671.30i -4.374 ± 1012.50i	-7.906 ± 376.94i -3.05 ± 697.10i -0.646 ± 725.77i -3.048 ± 1451.10i	Supersynchronous mode
-0.0003 ± 297.97i	± 297.97i	Torsional mechanical mode
-1.29 ±202.64i	-0.019 ± 202.83i	Torsional mechanical mode
-1.20±160.30i	-0.016 ± 160.48i	Torsional mechanical mode

-0.47 ± 126.69i	-0.006 ± 126.94i	Torsional mechanical mode
-18.255 ± 101.48i	-0.11 ± 98.547i	Torsional mechanical mode
-26.60 ± 33.21i	-4.732 ± 17.873i	
3.72 ± 83.46i	-5.738 ± 31.325i	Subsynchronous mode
-4.18 ± 257.79i		
-5.00 ±0.846i	-0.041 ± 14.327i	Swing mode
-1.081 ± 0.147i		
-0.001, -0.0886	-0.017, -0.704	
2.443, 16.051	-1.533, -13.728	
-20.498	-19.946, -25.495	Modes related to damper winding, field winding and SVC.
-54.271	-33.399, -48.837	
-94.63 -108.99	-106.420, -124.867	
-112.82, -1000.43	-952.364, -1000.023	

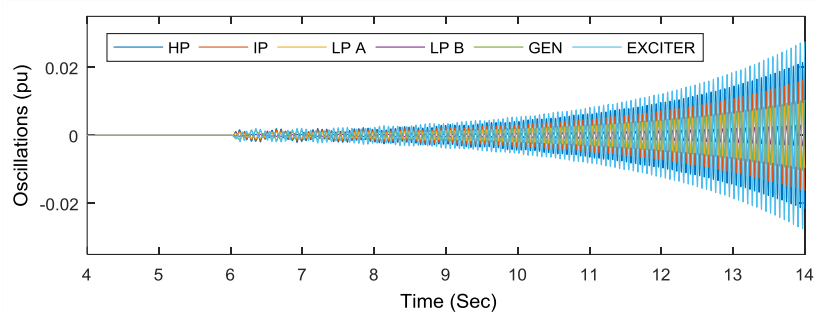

(a) Oscillations of masses.

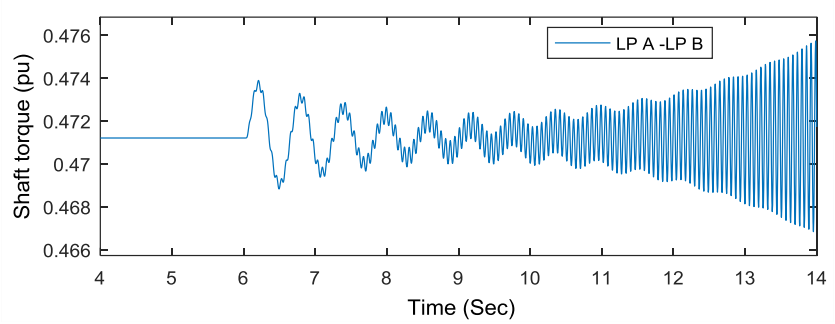

(b) LPA-LPB shaft torque for case III.

Fig. 8. Time domain simulation results.

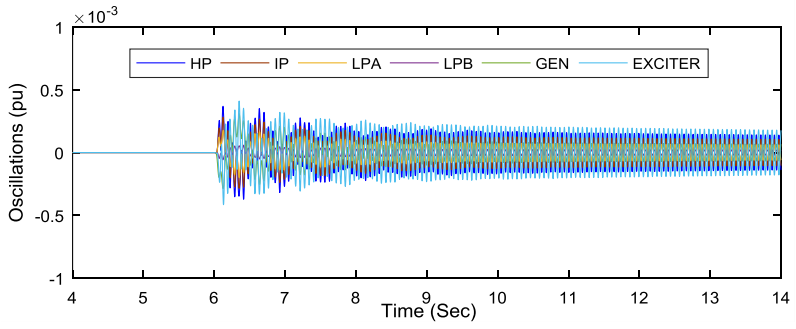

(a) Oscillations of masses.

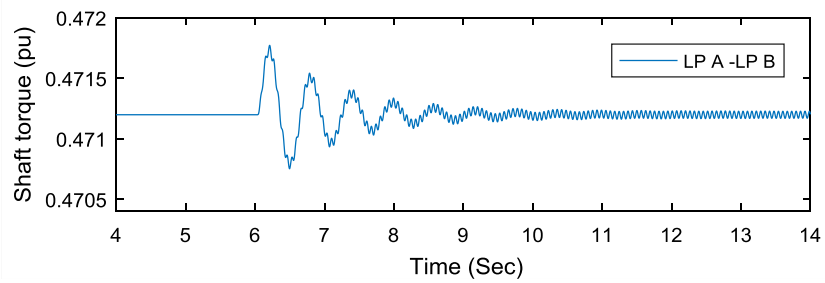

(b) LPA-LPB shaft torque for case IV.

Fig. 9. Time domain simulation results.

7. Conclusion

The paper presents the state space modelling of different electrical components to study SSR of IEEE FBM. The series compensation of transmission network with a certain degree of compensation may result in SSR. In this paper, an attempt is made to present a systematic approach to form the state space equation of IEEE FBM with different component modelling. For mitigating SSR, the modelling of the system with SSR is formulated and use of two supplementary feedback signals to operate SVC has been presented. Only SVC can't mitigate the subsynchronous resonance. As per case III, the use of AVR and PSS helps to improve the torsional modes of oscillations, but they resulted in lack of damping. The application of SVC with generator terminal voltage deviation as supplementary feedback signal has proved to be superior for mitigating SSR. The obtained results are strongly supported by the time domain simulation waveforms. In the presented work, the location of the series capacitor is at the far end of the transmission line but the interested reader can carry out further work by choosing any location of the series capacitor on the transmission line.

Nomenclatures

C_n	Capacitance of capacitor of SVC, farad (in per unit)
I_{2d}, I_{2q}	Current through series capacitor in d-q reference frame, pu amp
I_{3d}, I_{3q}	Current through TCR in d-q reference frame, pu amp
i_{cd}, i_{cq}	Generator stator current in d-q reference frame, pu amp
K_P, K_I	Proportional and integral control gain respectively
R	Resistance of transmission line, pu ohm
r_{fd}	Resistance of field winding, pu ohm
r_{kd}	Resistance of damper winding on d axis, pu ohm
r_{kq1}, r_{kq2}	Resistance of damper windings on q axis, pu ohm
r_s	Resistance of stator winding, pu ohm
T_1 ,T_2	Time delay for lag-lead network of PSS, second
T_3, T_4	Time delay for supplementary signal, second
T_D	Firing delay time, second
T_m	Measuring delay time, second
T_S	Average dead time, second

V_∞	Infinite bus voltage, pu volt
V_{1d}, V_{1q}	Voltage in d-q reference frame at SVC terminal, pu volt
V_{cd}, V_{cq}	Voltage across series capacitor in d-q reference frame, pu volt
V_{td}, V_{tq}	Generator terminal voltages in d-q reference frame, pu volt
x_{ad}	Direct axis reactance of synchronous machine, pu ohm
x_{aq}	Quadrature axis reactance of synchronous machine, pu ohm
X_C	Series compensation of transmission line, pu ohm
X_L	Inductive reactance of transmission line, pu ohm
x_{lfd}	Leakage reactance of field winding of synchronous machine, pu ohm
x_{lkd}	Leakage reactance of d axis rotor winding of synchronous machine, pu ohm
x_{lkq1}, x_{lkq2}	Leakage reactance of q axis rotor winding of synchronous machine, pu ohm
x_{ls}	Leakage reactance of stator winding of synchronous machine, pu ohm
x_{md}	Direct axis mutual reactance of synchronous machine, pu ohm

Greek Symbols

δ	Angular displacement of rotating mass (Fig. 1), radian
ψ	Flux linkages, weber
ψ_{ds}, ψ_{qs}	Stator flux linkages in d-q axis, weber
ψ_{ds0}, ψ_{qs0}	Initial values of stator flux linkages in d-q axis, weber
ψ_{fd}	Flux linkages of field winding, weber
ψ_{kd}	Flux linkages of damper winding on d axis, weber
ψ_{kq1}, ψ_{kq2}	Flux linkages of damper windings on q axis, weber
ω	Angular speed of rotating mass, rad/s.
ω_b	Base speed, rad/s.

Abbreviations

AVR	Automatic Voltage Regulator
FBM	First Benchmark Model
HP	High Pressure
IGE	Induction Generator Effect
PSS	Power System Stabilizer
SSR	Subsynchronous Resonance
SVC	Static Var Compensator
TCR	Thyristor Control Reactor
TI	Torsional Interaction

References

1. Ballance, J.W.; and Goldberg, S. (1973). Subsynchronous resonance in series compensated transmission lines. *IEEE Transactions on Power Apparatus and Systems,* PAS-92(5), 1649-1658.
2. IEEE Committee. (1977). First benchmark model for computer simulation of subsynchronous resonance. *IEEE Transactions on Power Apparatus and Systems,* 96(5), 1565-1572.

3. Anderson, P.M.; Agrawal, B.L.; and Ness, J.E.V. (1999). *Subsynchronous resonance in power systems* (1st ed.). New Jersey, United States of America: Wiley-IEEE Press.
4. Kundur, P. (2012). Power system stability and control (1st ed.). New York, United States of America: McGraw Hill, Inc.
5. IEEE SSR Working Group. (1980). Countermeasures to subsynchronous resonance problems. *IEEE Transactions on Power Apparatus and Systems*, PAS-99, 1810-1818.
6. Kumar, N.; and Kumar, S. (2014). Mitigation of SSR oscillations in series compensated line using LCAT subsynchronous damping controller. *TELKOMNIKA Indonesian Journal of Electrical Engineering*, 12(12), 8042-8050.
7. Padiyar, K.R.; and Varma, R.K. (1991). Damping torque analysis of static VAR system controllers. *IEEE Transactions on Power Systems*, 6(2), 458-465.
8. Larsen, E.V.; Rostamkolai, N.; Fisher, D.A.; and Poitras, A.E. (1993). Design of a supplementary modulation control function for the chester SVC. *IEEE Transactions on Power Delivery*, 8(2), 719-724.
9. Hammad, A.E.; and El-Sadek, M. (1984). Application of a thyristor controlled VAR compensator for damping subsynchronous oscillations in power systems. *IEEE Power Engineering Review*, PER-4(1), 44-45.
10. Hsu, Y.-Y.; and Wu, C.-J. (1988). Design of PID static VAR controller for the damping of subsynchronous oscillations. *IEEE Transactions on Energy Conversion*, 3(2), 210-216.
11. Wang, L.; and Hsu, Y.-Y. (1988). Damping of subsynchronous resonance using excitation controllers and static VAR compensators: A comparative study. *IEEE Transactions on Energy Conversion*, 3(1), 6-13.
12. Wasynczuk, O. (1981). Damping subsynchronous resonance using reactive power control. *IEEE Transactions on Power Apparatus and Systems*, PAS-100(3), 1096-1104.
13. Zhijun, E.; Fang, D.Z.; Chan, K.W.; and Yuan, S.Q. (2009). Hybrid simulation of power systems with SVC dynamic phasor model. *International Journal of Electrical Power and Energy System*, 31(5), 175-180.
14. Jovcic, D.; Pahalawaththa, N.; Zavahir, M.; and Hassan, H.A. (2003). SVC dynamic analytical model. *IEEE Transactions on Power Delivery*, 18(4), 1455-1461.
15. Jusan, F.C.; Gomes Jr, S.; and Taranto, G.N. (2010). SSR results obtained with a dynamic phasor model of SVC using modal analysis. *International Journal of Electrical Power and Energy Systems*, 32(6), 571-582.
16. Zhu, X.; Jin, M.; Kong, X.; Zhao, J.; Liu, J.; and Zhao, Q. (2018). Subsynchronous resonance and its mitigation for power system with unified power flow controller. *Journal of Modern Power Systems and Clean Energy*, 6(1), 181-189.
17. Panda, S.; Baliarsingh, A.K.; Mahapatra, S.; and Swain, S.C. (2016). Supplementary damping controller design for SSSC to mitigate sub-synchronous resonance. *Mechanical Systems and Signal Processing*, 68-69, 523-535.

18. Nagarajan, S.T.; and Kumar, N. (2015). Fuzzy logic control of SVS for damping SSR in series compensated power system. *International Transactions on Electrical Energy Systems*, 25(9), 1860-1874.
19. Sreeranganayakulu, J.; Marutheswar, G.V.; and Anjaneyulu, K.S.R. (2016). Mitigation of sub synchronous resonance oscillations using static VAR compensator. *Proceedings of the International Conference on Electrical, Electronics and Optimization Techniques (ICEEOT).* Chennai, India, 4145-4153.
20. Krause, P.C.; Wasynczuk, O.; and Sudhoff, S.D. (2002). *Analysis of electric machinery and drive systems* (2nd ed.). New Jersey, United States of America: John Wiley & Sons, Inc.

Appendix A

Synchronous machine parameters for IEEE-FBM: Values are in pu X_T=0.14 pu, R_L=0.02, X_L=0.50, X_{SYS}=0.06, X_C=0.371, P_g=0.9, V_T=1.

Reactance	Value (pu)	Time constant	Value (sec)
Xd	1.79	T'd0	4.3
X'd	0.169	T"d0	0.032
X"d	0.135	T'q0	0.85
Xq	1.71	T"q0	0.05
X'q	0.228		
X"q	0.2		
Xad	0.13		

Mechanical masses value IEEE-FBM.

Inertia	Inertia constant (H)	Shaft section	Spring constant (K) in pu torque/rad
HP turbine	0.092897	HP-IP	19.303
IP turbine	0.155589	IP-LPA	34.929
LPA turbine	0.85867	LPA-LPB	52.038
LPB turbine	0.884215	LPB-GEN	70.858
Generator	0.868495	GEN-EXC	2.82
Exciter	0.034217		

Parameters of different control circuit.

Parameter	K_P	K_I	K_D	T_S	T_D	T_M	B
Value	0.3	30	0.05	0.02066	0.008	0.001	1 pu

Parameter	T_R	K_F	K_A	T_F	T_A	K_R	X_{Cn}
Value	0.01	0.058	30	0.62	0.04	30	1 pu

Parameter	T_1	T_2	T_3	T_4	K_B	K_{STAB}	T_W
Value	0.154	0.033	0.001	0.03	0.065	10	1.4

Appendix B

$$[A_e]=\begin{bmatrix}
\frac{r_s\omega_b}{x_{ls}}\left(\frac{x_{aq}}{x_{ls}}-1\right) & -\omega_0 & \frac{r_s\omega_b}{x_{ls}}\left(\frac{x_{aq}}{x_{lkq1}}\right) & \frac{r_s\omega_b}{x_{ls}}\left(\frac{x_{aq}}{x_{lkq2}}\right) & 0 & 0 \\
\omega_0 & \frac{r_s\omega_b}{x_{ls}}\left(\frac{x_{ad}}{x_{ls}}-1\right) & 0 & 0 & \frac{r_s\omega_b}{x_{ls}}\left(\frac{x_{ad}}{x_{lfd}}\right) & \frac{r_s\omega_b}{x_{ls}}\left(\frac{x_{ad}}{x_{lkd}}\right) \\
\frac{r_{kq1}\omega_b}{x_{lkq1}}\left(\frac{x_{aq}}{x_{ls}}\right) & 0 & \frac{r_{kq1}\omega_b}{x_{lkq1}}\left(\frac{x_{aq}}{x_{lkq1}}-1\right) & \frac{r_{kq1}\omega_b}{x_{lkq1}}\left(\frac{x_{aq}}{x_{lkq2}}\right) & 0 & 0 \\
\frac{r_{kq2}\omega_b}{x_{lkq2}}\left(\frac{x_{aq}}{x_{ls}}\right) & 0 & \frac{r_{kq2}\omega_b}{x_{lkq2}}\left(\frac{x_{aq}}{x_{lkq1}}\right) & \frac{r_{kq2}\omega_b}{x_{lkq2}}\left(\frac{x_{aq}}{x_{lkq2}}-1\right) & 0 & 0 \\
0 & \frac{r_{fd}\omega_b}{x_{lfd}}\left(\frac{x_{ad}}{x_{ls}}\right) & 0 & 0 & \frac{r_{fd}\omega_b}{x_{lfd}}\left(\frac{x_{ad}}{x_{lfd}}-1\right) & \frac{r_{fd}\omega_b}{x_{lfd}}\left(\frac{x_{ad}}{x_{lkd}}\right) \\
0 & \frac{r_{kd}\omega_b}{x_{lkd}}\left(\frac{x_{ad}}{x_{ls}}\right) & 0 & 0 & \frac{r_{kd}\omega_b}{x_{lkd}}\left(\frac{x_{ad}}{x_{lfd}}\right) & \frac{r_{kd}\omega_b}{x_{lkd}}\left(\frac{x_{ad}}{x_{lkd}}-1\right)
\end{bmatrix}$$

$$B_{eN}=\begin{bmatrix}\omega_b & 0 & 0 & 0 & 0 & 0\\ 0 & \omega_b & 0 & 0 & 0 & 0\end{bmatrix}^T$$

$$B_{eM}=\begin{bmatrix}-\psi_{ds0} & \psi_{qs0} & 0 & 0 & 0 & 0\end{bmatrix}^T$$

$$B_{eP}=\begin{bmatrix}0 & 0 & \omega_b & 0 & 0 & 0\\ 0 & 0 & 0 & \omega_b & 0 & 0\\ 0 & 0 & 0 & 0 & \frac{\omega_b r_{fd}}{x_{md}} & 0\\ 0 & 0 & 0 & 0 & 0 & \omega_b\end{bmatrix}^T$$